Master of Science

DEFORMATION AND FRACTURE
OF A METAL MATRIX COMPOSITE
MODEL SYSTEM

BY

KENNETH ERICSON FUSCH

Course I   June/1968

DEFORMATION AND FRACTURE
OF A METAL MATRIX COMPOSITE
MODEL SYSTEM

by

KENNETH ERICSON FUSCH
BS, United States Naval Academy
(1964)

Submitted in partial fulfillment
of the requirements for the degree of

Master of Science in Civil Engineering

at the
Massachusetts Institute of Technology

(June 1968)

ABSTRACT

DEFORMATION AND FRACTURE
OF A METAL MATRIX COMPOSITE
MODEL SYSTEM

by

KENNETH ERICSON FUSCH   ,

Submitted to the Department of Civil Engineering on 17 May
1968 in partial fulfillment of the requirements for the
degree of Master of Science in Civil Engineering.

A continuous-fiber metal matrix composite model system
is experimentally developed by combining large diameter
(1/16") stainless steel fibers, or rods, with a matrix of
high purity aluminum. The model system is designed to
compare closely with actual composite systems in the
following ways: (1) stress-strain behavior, (2) mode of
failure, (3) theoretical predictions of strength, and (4)
the development of fiber tensile stress through matrix shear
stress transfer.

The critical aspect ratio for the model system is
determined by using the pull-out load method. Both 3-fiber
and 5-fiber models are fabricated by a gravity casting tech-
nique. Mechanical testing of specimens is carried out in
tension parallel to the fiber axis.

Deformation of the pure aluminum matrix is studied
through direct microhardness measurements of strain harden-
ing. Qualitative analysis of the stress-strain behavior and
the fracture mode is also made.

Results show that the model systems exceed rule-of-
mixtures strength predictions, thereby indicating that
synergistic effects are present. Microhardness test results
verify the existence of high levels of matrix shear stress
near the fiber ends.

Thesis Supervisor: Russel C. Jones, Ph.D.

Title: Associate Professor of Civil Engineering

ACKNOWLEDGMENTS

TABLE OF CONTENTS

I.   INTRODUCTION

General

The development of filamentary materials with
extremely high strengths and stiffnesses has given impetus
to the growth of the field of composite materials. Strong
fibers have been successfully combined with matrix materials
of a dissimilar nature to produce new products with superior
mechanical properties.

The use of a metallic matrix gives many advantages
over non-metallic matrices, among these being improved
high-temperature performance. The plastic flow character-
istics of a metal matrix provide a means for efficient
stress transfer between fibers and a reduction in the
notch-sensitivity of the composite [1]*. The ability of a
metal matrix to strain harden introduces still another
improvement in overall composite performance. Lightweight
metallic matrices have the added benefit of allowing
fabrication of fibrous composites with high specific
strengths and stiffnesses.

Metal matrix composites hold great potential for
future engineering applications. The aerospace industry
which places a premium on high strength/lightweight

---

* Numbers in brackets refer to references listed at the
  end of this report.

materials has been first to capitalize on the early develop-
ment of fiber-reinforced metals.

Current research is being conducted on two fronts:
(1) the improvement of fabrication techniques, coupled with
an attempt to understand more fully how fabrication variables
affect the final product, and (2) a better understanding of
the mechanics, both micro- and macro-, of composite behavior.
Two drawbacks are apparent at this stage of composite de-
velopment. The anisotropic nature of fibrous composites
places limitations on structural applications, and the high
cost of these materials places the product out of economic
reach for many applications. Current high costs, however,
are due primarily to the initial research and development
efforts, and significant price reductions can be anticipated
in the future.

The earlier development of fiber-reinforced plastics
has provided a bonus for investigators in the field of metal
matrix composites. Many techniques of experimental research
used in fiber-reinforced plastics, as well as much of the
basic theoretical work, can be utilized in the expanding
metal matrix composite research effort. However, the
markedly different characteristics of metallic and non-
metallic matrices have called for some modifications to the
theoretical picture and for new experimental approaches.
Much work in fiber-reinforced plastics has involved the use

of birefringent resin matrices to study the principles of composite action - a technique which obviously cannot be carried over to metal matrix composites. New approaches have been devised, however, and many more are in the planning stages. A successful approach to studying the plastic deformation characteristics of ductile metallic matrices has involved the measurement of matrix strain hardening through the use of direct microhardness techniques.

Use of Model Systems

Sutton [2] has classified studies on fiber-reinforced metals into the following two categories: "(1) those dealing with the careful preparation of model composite systems to modify or extend existing theories, and (2) those dealing with various metals and alloys reinforced with both metallic and ceramic fibers to develop useful engineering materials." In the latter category, numerous investigators [3,4,5] have published papers discussing the fabrication and performance of specific metal matrix composite systems. Although these research efforts are not elaborated upon herein, it is important to note that the aluminum/stainless steel composite discussed by Davis [6] serves as a reference point for the model system developed and studied in this research effort.

The use of metal matrix composite model systems has provided the basis for much of the presently accepted theory on composite strength and behavior. Model systems have been used extensively because (1) better control over fabrication variables can be maintained and (2) more success in isolating, or separating, experimental parameters can be achieved. Such problems as fiber alignment, interfiber spacing and eccentricity of loading can be minimized or overcome through model techniques. Stress concentrations due to various fiber end geometries in discontinuous-fiber composites can be handled more effectively through the use of single-fiber model systems. The effects of metallurgical reactions between fiber and matrix resulting from various fabrication processes can be studied in greater detail through model systems. Burte et al [7] have studied the various interactions that can occur during composite fabrication and/or subsequent elevated temperature exposure with model systems in which the metals used for fiber and matrix were selected on the basis of metallurgical considerations, rather than ultimate mechanical performance.

Another approach with model systems involves the study of the micromechanics of fibrous composite behavior. Experimental work by Ebert et al [8] has employed model systems of both densely-packed and loosely-packed multi-filament composites to develop design criteria for composite

materials. The work of Ebert considers such problems as the effects of residual stresses due to differences in coefficients of thermal expansion and the occurrence of a triaxial stress state in both fiber and matrix during uniaxial loading.

Many composite model systems which have been studied to date have been fabricated with materials that have been selected for reasons of experimental convenience. Material combinations which have minimal chemical reactions, compatible coefficients of thermal expansion, or good surface wetting characteristics have often been chosen. The result has been the development of model systems which are non-practical composites. Although these model systems have been beneficial in formulating basic composite theory, their usefulness in solving practical problems is often limited. The materials used in this model study have been chosen in an attempt to circumvent this limitation. It is anticipated that the carry-over from model system performance to actual composite development will be enhanced through the use of an aluminum/stainless steel system.

The use of an array of large diameter fibers in a metallic matrix represents a new approach to modeling techniques. The use of small-scale models is not new; structural engineers have used this method for years to gain insight into the performance of actual structures. However, the

use of large-scale models in materials science is a relatively new concept. Ebert's work involves just such an approach. It is expected that a better understanding of the macromechanics of scaled-up models will shed significant light on the micromechanics of actual composite systems.

The metal matrix composite model system of this research effort is a large diameter, continuous-fiber system. Continuous fibers, with a diameter roughly one order of magnitude larger than the diameter of many commercially available fibers used in composite fabrication, are used in conjunction with an extremely ductile matrix, high purity aluminum. Although the strength properties of the large diameter fibers, or rods, are much lower than the corresponding values for typical metallic fibers found in practical composites, the use of low strength pure aluminum as the matrix maintains good correlation between fiber properties and matrix properties.

The object of this work has been twofold: (1) to develop a useful continuous-fiber metal matrix composite model system and (2) to study the deformation and fracture characteristics of such a model system. The validity of the model system is based on the following criteria:

    (1)   stress-strain behavior
    (2)   mode of failure
    (3)   theoretical predictions of strength
    (4)   the development of fiber tensile stress through matrix shear stress transfer

To be a valid model, the system developed must compare closely with actual composite systems in each of these categories.

II. MODEL SYSTEM DESIGN

The Pull-Out Load Method

In order to ensure proper composite behavior in the
continuous-fiber model systems, it was necessary to determine
the critical length of fibrous reinforcement, i.e., the min-
imum length of fiber which must be embedded in the matrix.
Only when the length of fibrous reinforcement equals or ex-
ceeds this critical length will there be sufficient fiber-
matrix interfacial area to cause fiber fracture through the
mechanism of shear stress transfer. Weeton and Signorelli
[9] discuss the process of fiber-matrix load transfer for
both continuous and discontinuous fibers. The critical
length, L_c, has been shown to be a function of fiber
diameter, D; the ultimate tensile strength of the fiber,
δ_f; and the shear strength of the interfacial bond or the
shear strength of the matrix, τ, whichever is less. This
relationship, in terms of the critical aspect ratio,
$\frac{L_c}{D}$, is given by

$$\frac{L_c}{D} = \frac{1}{4} \frac{\delta_f}{\tau}$$ (Eq. 1)

This expression serves as the basis of an experimental
method of determining the critical aspect ratio. This

method is the single-fiber pull-out load test. There are
certain drawbacks, however, to the use of the pull-out test.
Since only a portion of the fiber is embedded in the matrix,
tensile load is applied directly to the fiber rather than
through interfacial shear stresses along the entire fiber
axis as would be the case in an actual composite [10]. In
addition, the use of a single fiber does not take into
account the influence of surrounding fibers [11]. Regard-
less of these limitations, the method has been used by
numerous investigators and it appears to be sound at least
qualitatively.

The pull-out test is based upon the concept that fibers
embedded in a matrix material to depths less than half the
critical length, $\frac{L_c}{2}$, will pull-out, whereas fibers em-
bedded to depths greater than $\frac{L_c}{2}$ will fracture. Thus,
the critical length is established as twice the depth at
which pull-out ceases to be the mode of failure and fiber
fracture begins. The use of equation (1) will give an indi-
cation of the degree of bonding between fiber and matrix.
However, this relationship cannot be used to obtain precise
values of interfacial or matrix shear strength due to the
nonuniformity of the shear stress distribution along the
fiber axis. It is more realistic to assume that the value
of τ obtained from equation (1) is an average interfacial
shear stress. The nonuniformity of the interfacial shear

stress is shown more clearly in Figure 1, which is a schematic representation of the shear stress distribution along the fiber axis for various lengths of fiber embedded in the matrix. The build-up of fiber tensile stress is also plotted. The assumption of a linear tensile stress build-up along the fiber is supported by Kelly and Davies [12].

Stainless steel fibers ($\frac{1}{16}$" diameter) were embedded in pure aluminum at various depths ranging from $\frac{5}{8}$" to almost 4". Pull-out tests were conducted on an Instron testing machine at a crosshead rate of 0.1 inches per minute. Blunted end fibers were used in all pull-out specimens. Figure 2 shows a sample pull-out specimen prior to testing. Gripping of specimens in the Instron testing machine was done in such a manner that no lateral restaint was exerted upon the fiber during testing. Shown in Figure 3 is a plot of failure load (maximum pull-out load) vs. length/diameter ratio for stainless steel fibers in pure aluminum.

It is apparent from the data in Figure 3 that the results of the pull-out tests can be used to establish the critical aspect ratio. A definite change in failure mode was observed at a length/diameter ratio of 36. It is also apparent that the results for the test specimens that failed by fiber pull-out (less than half the critical length embedded) do not agree with the theoretical expectations as shown by the dashed line. This theoretical curve is based

upon the assumption of a uniform interfacial shear stress distribution along the fiber axis. It further assumes that the blunted end fiber is unbonded to the matrix. The data suggest a parabolic, rather than linear, relationship in this region. This behavior can be explained by (1) matrix strain hardening and (2) high interfacial or matrix shear stresses near the fiber ends.

The stress-strain behavior of the high purity aluminum matrix is such that plastic flow occurs at low levels of stress. Associated with this plastic flow is strain hardening. As tensile load is applied to the fiber during the pull-out test, plastic flow takes place in the matrix in the vicinity of the fiber. This transfer of stress is brought about by the interfacial bonding between fiber and matrix. As the matrix flows, strain hardening produces an increase in the resistance to fiber pull-out. This caused a higher maximum pull-out load than would have been recorded if no matrix strain hardening occurred. Evidence to support this has been obtained through direct microhardness techniques. An increase in Vicker's Hardness Number from 20.7 to 22.9 was found in the pure aluminum matrix adjacent to the fiber cavity after pull-out testing. This increase was not as large at distances of $\frac{1}{2}$ fiber diameter and 1 fiber diameter away from the cavity.

The fiber-matrix interaction has been shown to manifest itself in high values of shear stress near fiber ends

[13,14]. These high shear stresses are present even when
the fiber length is less than critical; hence, the resistance
to fiber pull-out is greater than would be anticipated if the
interfacial or matrix shear stresses were constant along the
fiber axis. (Refer to Figure 1).

An additional reason for the high pull-out loads (for
the case where less than half the critical length is embedded)
is bonding at the fiber ends. Although this is probably a
minor cause for the high loads, it is interesting that
Kelly and Tyson [15] have noted that "there is an appre-
ciable stress transferred across the fiber end for specimens
with the end bonded to the matrix."

Development of Model Design

The final design of the continuous-fiber metal matrix
composite system was based upon the experimental determina-
tion of the critical aspect ratio and upon a method of ten-
sile loading that (1) would assure proper composite stress-
strain behavior and that (2) would develop the ultimate
tensile strength of the fibers through the transmission of
shear stress through the matrix, rather than through any
direct tensile stress on the fibers. A circular cross-
section was ultimately selected to aid in model fabrication
during machining operations. Design of the circular cross-
section for the 3-fiber and the 5-fiber models used in this

study is shown in Figure 4.

Initial plans for conducting tensile tests of the
continuous-fiber models called for the ends of the test
specimens to be held with conventional grips which exert
lateral restraining forces on the specimen ends, as shown
schematically in Figure 5A. Two reasons can be cited as
justification for abandoning such conventional grips for
shoulder grips: (1) the extreme ductility of the pure
aluminum matrix and (2) the desire to introduce tensile
stresses in the fibers solely through the action of shear
stress transfer through the matrix, rather than through
artificial means. At this stage, design of the model
system was modified as shown in Figure 5B. (Note the
arrows which indicate the nature of the tensile loading).
The specimen length between points of load application was
set at L_c to guarantee that adequate tensile stress would
be built up within the fibers to cause fracture. Several
3-fiber models were fabricated according to this design.
Subsequent tensile testing revealed that this modified
design did not work properly, i.e., the mode of failure was
a matrix shear failure with no fiber fracture occurring.
Photographs of the failure mode of several of these
improperly designed specimens are shown in Figure 6.

A further modification in model design was introduced
at this point. The alteration involved a change in the

points of load application such that one-half of the

critical length was outside of the loading points as

illustrated in Figure 5C. This final modification worked

satisfactorily and both the 3-fiber and 5-fiber models were

designed accordingly. Figure 7 shows the final model

system design prior to testing and after fracture.

III. FABRICATION OF MODEL SYSTEMS

Selection of Materials

The model systems used in this research effort have
been composed of 1/16" diameter stainless steel fibers in
a matrix of pure aluminum. The choice of stainless steel
and aluminum for the fibers and matrix, respectively, was
based upon two reasons: (1) stainless steel/aluminum compos-
ites are currently available commercially; hence a good
reference exists for making comparisons between actual metal
matrix composite behavior and the model system behavior;
(2) low cost and availability of materials. The steps used
in fabricating a commercial 2024 aluminum/NS355 stainless
steel (.009 inch diameter fibers) composite are described in
detail by Sumner [16].

The aluminum used as the matrix had a purity of 99.99%.
The use of this high purity aluminum was desirable because
of its high ductility, low strength, and good strain
hardening characteristics. Mechanical testing revealed an
ultimate tensile strength of 6600 psi., a yield strength
(0.2% offset) of 2900 psi. and an elongation in 2" of 50%.
These values agree closely with published mechanical prop-
erties for this grade of high purity aluminum [17].

The selection of aluminum as the matrix metal seemed
warranted in view of its high potential usefulness as a matrix

in future commercial applications. Such characteristics
as no ductile-brittle transition and low load-rate sensi-
tivity, coupled with its light weight and low cost, make
aluminum and its alloys very attractive as metallic matrices.

AISI type 304 stainless steel in 1/16" diameter rods
(fibers) was selected for use in this experimental work.
Type 304 is an austenitic stainless steel with the following
approximate chemical composition [18]: 18-20% Cr, 8.0-12.0%
Ni, 0.08% C, 1.0% Si, 2.0% Mn, 0.045% P, and 0.03% S.
Typical mechanical properties include an ultimate tensile
strength of 127,000 psi., a yield strength (0.2% offset) of
93,000 psi., and an elongation of 2" of 47%. The choice of
an austenitic stainless steel over a martensitic stainless
steel was based upon a higher elongation in the former. The
use of a ferritic stainless steel did not seem desirable due
to the possibility of 885°F embrittlement during the high
temperature fabrication procedure used in this work.

The use of extremely ductile fibers is actually a
limitation of the model system, although it is an experi-
mental necessity. The high strength fibers used in most
metal matrix composites are relatively brittle. The high
degree of ductility (measured by fiber elongation) was
necessary to ensure that the fiber volume fraction in the
continuous-fiber model systems would exceed both the minimum
volume fraction and the critical volume fraction which are

defined by Broutman and Krock [19] in the following manner:

$$V_{f_{crit.}} = \frac{\delta_{mu} - (\delta_m)_{\varepsilon'_f}}{\delta^*_{fu} - (\delta_m)_{\varepsilon'_f}} \qquad \text{(Eq. 2)}$$

$$V_{f_{min.}} = \frac{\delta_{mu} - (\delta_m)_{\varepsilon'_f}}{\delta^*_{fu} + \delta_{mu} - (\delta_m)_{\varepsilon'_f}} \qquad \text{(Eq. 3)}$$

where, δ_{mu} = ultimate tensile strength of the metallic matrix,

  δ^*_{fu} = ultimate tensile strength of the fibers,

  $(\delta_m)_{\varepsilon'_f}$ = matrix stress when the fibers are strained to their ultimate tensile strain.

The volume fraction of fibers, V_f , in a metal matrix composite must exceed $V_{f_{crit.}}$ if fiber strengthening is to occur, i.e., if the ultimate tensile strength of the composite, δ_{cu} , is to exceed the strength of the strain hardened matrix alone. V_f must exceed $V_{f_{min.}}$ if the strength of the composite is to be found from the following rule-of-mixtures relationship:

$$\delta_{cu} = \delta^*_{fu} V_f + (\delta_m)_{\varepsilon'_f} (1 - V_f) \qquad \text{(Eq. 4)}$$

The use of high ductility stainless steel fibers in the
model systems results in low values of $V_{f_{min.}}$ and
$V_{f_{crit.}}$. Because the ultimate tensile strain of the fibers
is very high, the stress in the matrix at the point of fiber
fracture is only slightly less than the ultimate tensile
stress of the matrix. Thus the numerators of both equations
(2) and (3) are quite small, giving rise to negligible values
of $V_{f_{min.}}$ and $V_{f_{crit.}}$.

The limitation imposed by the use of very ductile fibers
does not reduce the validity of the model system significantly
since the fibers in some commercial composites fracture in a
ductile fashion. The scanning electron micrograph shown in
Figure 22 clearly shows a classical cup-and-cone fracture
mode for the fibrous reinforcement. To circumvent this
ductile fiber limitation, a martensitic stainless steel such
as AISI type 416 (with a fiber elongation of only 10-30%)
might be employed in a similar model design. However, this
would require that the model system volume fraction be
somewhat higher in order to exceed $V_{f_{min.}}$ and $V_{f_{crit.}}$.

Model Fabrication

Both the continuous-fiber models and the pull-out test
specimens were fabricated by using a gravity casting tech-
nique. This technique involved pouring molten aluminum into
graphite molds containing the stainless steel fibers.

The two graphite mold designs used for casting were as
follows: (1) a vertical circular mold for continuous-fiber
models and (2) a horizontal rectangular mold for the pull-
out test specimens. The molds are pictured in Figure 8.
Grade CS graphite was used for both molds.

All castings were done in an air environment with the
molds and the stainless steel fibers at room temperature
prior to the introduction of the molten aluminum into the
molds. Pure aluminum in ingot form was placed in a crucible
and then heated to its melting point (660°C) in a laboratory
furnace. The molten aluminum was next heated to a temperature
of 1000°C before pouring. The reasons for this additional
heating above the melting point were (1) to ensure molten
aluminum flow around the fibers in the model systems before
solidification began and (2) to improve the quality of the
fiber-matrix bonding by promoting some metallurgical inter-
action.

Preliminary investigations revealed that some surface
preparation of the 1/16" stainless steel fibers was necessary
to ensure an acceptable degree of bonding during fabrication.
Accordingly, the following three-step fiber cleaning opera-
tion was employed to aid in the removal of oxide layers, oil
and grease films, and other unwanted debris:

    (1) rubbing with emery cloth
    (2) 1 minute agitation in methanol (methyl alcohol)
    (3) 1 minute

Upon completion of fiber cleaning, the stainless steel
fibers were arranged in the appropriate graphite mold and
the 1000°C molten aluminum was poured into the mold. The
molten aluminum was then allowed to solidify and to continue
cooling in air until the model system casting reached room
temperature. This relatively slow cooling of the model
system was permitted so as to take advantage of solid state
diffusion which occurs at high temperatures in an attempt to
improve fiber-matrix bonding. Slow cooling also assured a
large grain size in the matrix as can be seen in Figure 9.
This large grain size was necessary so that the mean grain
diameter would be on the same order of magnitude as the fiber
diameter and hence increase the validity of the model system.
This relationship between approximate matrix grain size and
fiber diameter is found in many commercial composites such
as the aluminum/stainless steel composite used as a reference
point.

After the model composites reached room temperature, they
were removed from the graphite molds in preparation for
machining. Figure 10 shows a continuous-fiber model and a
pull-out test specimen in the as-cast condition. All model
systems and pull-out specimens were machined into the appro-
priate shapes for mechanical testing through the use of a
conventional lathe and a horizontal milling machine. Figure
11 is a scaled drawing of both a pull-out test specimen and

a continuous-fiber model.

Effects of Fabrication on Fiber Properties

The fabrication of metal matrix composites often
involves processes that alter the mechanical properties of
the fibrous reinforcement. This alteration of fiber prop-
erties may or may not enhance the performance of the compos-
ite. Sutton [2] discusses this problem, pointing out that
considerable care must be exercised during all stages of
fabrication to ensure that fibers are not damaged or
weakened. Brittle fibers such as boron and silica are quite
susceptible to fracture during such operations as cold
rolling or hot pressing. Ductile fibers are less prone to
fracture during these operations; however all fibrous
reinforcement is subject to degradation through combinations
of chemical reaction and/or diffusion. Exposure to high
temperature environments can change the mechanical properties
of metallic fibers through the process of annealing or by
various types of embrittlement.

The method used in fabricating the continuous-fiber
aluminum/stainless steel model systems discussed herein
involves the casting of molten aluminum around stainless steel
fibers, thereby subjecting the fibers to a high-temperature
environment for a substantial period of time. To gain some
insight as to how the fiber properties are affected by this

high-temperature environment, a plot of fiber temperature
vs. time in the fabrication process was determined as
shown in Figure 12. To obtain accurate data for this plot,
a chromel-alumel thermocouple was placed in the center of a
graphite mold. This was accomplished by sliding the thermo-
couple wires into two small holes in a 1/8" hole in the end
of the graphite mold in such a manner that the chromel-
alumel junction occupied a position at the center of the mold.
Molten aluminum heated to 1000°C was poured into the mold and
allowed to solidify and cool around the thermocouple. Temper-
ature readings were taken at specified intervals of time.

The primary concern with type 304 stainless steel was
a possible change in its mechanical properties through the
process of annealing. Austenitic stainless steels are
annealed at temperatures between 950°C and 1100°C [18].
Since the fiber temperatures dropped below this annealing
range almost immediately, it is assumed that negligible
change in the fiber mechanical properties took place. To
further substantiate this assumption, type 304 stainless
steel fibers were heated for 30 minutes at temperatures
ranging from 800°C to 1000°C. The results of mechanical
testing of these specimens indicated that an average ultimate
strength reduction of only 12% occurred due to this exces-
sive heating. Fiber elongation did not increase appreciably
until the temperature reached 1000°C for the 30 minute
period.

Optical microscopy indicated that there was no for-
mation of an interfacial third phase around the fibrous
reinforcement as a result of the elevated temperature fabri-
cation process.

IV. DEFORMATION AND FRACTURE

Stress-Strain Behavior

In order to study the deformation and fracture characteristics of the large fiber metal matrix composite model system, the 3-fiber and 5-fiber models were subjected to tensile loading parallel to the fiber axis. Loading was carried out through the use of an Instron testing machine at a crosshead rate of 0.1 inches per minute. It is important to recall that the manner of loading developed herein applies no direct tensile stresses to the fibers; fiber tensile stress is generated indirectly through the mechanism of shear stress transfer through the matrix.

Kelly and Davies [12] postulate that the stress-strain behavior of metal matrix composites can be divided into the following four stages:

Stage I.   Elastic deformation of both fiber
           and matrix

Stage II. Fiber elastic, but matrix now plastic

Stage III. Plastic deformation of both fiber
           and matrix

Stage IV. Fiber fracture followed by matrix
           failure

This four-stage behavior is supported by the performance under tensile stress of both tungsten fiber-copper matrix composites and stainless steel fiber-aluminum matrix composites. Figure 13 shows the four stages of composite deform-

tion schematically. A theoretical analysis of ideal fiber-reinforced composites by MacFadyen and Jones [20] agrees with this stress-strain behavior.

Practical considerations arising with the type of loading used for the 3-fiber and 5-fiber models prohibited an accurate measurement of strain during the loading process. Figure 14 shows one end of a model system in a shoulder grip. Hence, the determination of a stress-strain curve for the models was not possible. Load-deformation curves for the model systems are shown in Figures 15 and 16. These curves indicate that four-stage composite behavior does occur for both model systems. The end of stage III deformation for fiber-reinforced composites is marked by fracture of the high-strength fibers. This point is shown distinctly on the load-deformation curves. Stage I terminates when the matrix ceases to behave elastically. This point is also revealed in Figures 15 and 16. The transition from stage II to stage III is less pronounced, however this is characteristic of fibrous composites reinforced with ductile fibers.

Matrix Deformation

The strain hardening characteristics of the metallic matrix play an important role in the overall performance of a

metal matrix composite. Plastic flow of the metal matrix serves as the primary means of shear stress transfer in fibrous composites and it can produce considerable strain hardening. The elastic-plastic transition in high purity aluminum occurs at very low levels of stress, hence strain hardening begins early in the stress-strain life of composites fabricated with pure aluminum matrices. A technique for studying the plastic deformation of metallic matrices, and thus the level of stress, has been used by Jones [21]. This technique involves the determination of the amount of strain hardening by direct microhardness measurements. This method has been used by Parikh [13] to verify the existence of high levels of stress near fiber ends by experimentation with a single short tungsten fiber in a silver matrix.

The experimental procedure used involved the determination of the Vicker's Hardness Number for various key locations in the model systems. As reference points for microhardness testing, the Vicker's Hardness Number was obtained for uncomposited pure aluminum in both an unstressed condition and after tensile failure. The average H_v for the unstressed aluminum was 20.7; the average H_v for the aluminum loaded in tension until fracture was 30.4. These two values of H_v represent the lower and upper bounds of microhardness for pure aluminum. Thus, a 50% increase in microhardness can be realized in pure aluminum in going from an unstressed to a

-52-

fractured condition.

After mechanical testing of the model systems had been completed, the test specimens were sectioned in such a manner as to expose various critical areas in which microhardness readings were to be taken. Sectioning of specimens was accomplished by a spark erosion cutting process so as to minimize any additional plastic deformation of the exposed surfaces as would occur with standard mechanical cutting procedures. All cutting was done with a Servomet spark cutter using the finest cutting rate available (no. 7). Specimen surfaces were then electropolished with a perchloric acid solution to remove any surface deformation caused by spark cutting and to produce a relatively smooth surface for making microhardness indentations.

A Leitz microhardness tester was employed to make microhardness indentations. The Vicker's Hardness Number at designated locations was determined by making a series of four diamond indentations as shown in Figure 17. The average value of H_v for the cluster of four indentations thus gives an indication of the amount of strain hardening in the aluminum matrix at areas of interest. Figure 18 shows the areas on a longitudinal section where microhardness readings were taken. Readings were taken at each of the following radial distances from the fibers:

(1) Immediately adjacent to fiber – both within the fiber cage (interior) and

outside (exterior)

(2)   1/2 fiber diameter away

(3)   1 fiber diameter away

The results of the microhardness testing are shown in
Figure 19 in which H_V is plotted against fiber length.
Values plotted are for readings taken adjacent to the fiber
on both interior and exterior sides. The high values of H_V
in locations 1 and 2 can be explained on the basis of
proximity to the point of final matrix failure. A decrease
in hardness in locations 3 and 4 seems consistent in view of
increasing distance from the point of matrix failure. An
increase in hardness was found in locations 5 and 6. This
evidence of large amounts of plastic deformation agrees well
with the high level of matrix shear stress in this area
necessary to generate sufficient tensile stress in the fiber
to cause fracture. (Refer to Figure 1). Although the hard-
ness values in Figure 19 are slightly higher for the interior
case than for the exterior case, both curves exhibit the same
general behavior. The discrepancy in hardness values is
within the experimental error associated with microhardness
testing. Values of H_V in the matrix as a function of radial
distance from the fiber are relatively constant. This finding
substantiates the work of Jones [21] in which he reported that
the shear stress transfer in the matrix does not involve
appreciably higher strains in the immediate vicinity of the
fibers.

To obtain more information about the matrix strain hardening characteristics at various critical locations on the cross-section, both the 3-fiber and 5-fiber models were sectioned perpendicular to the fiber axis approximately half the distance between the point of load application and the fracture surface. A high degree of hardness, indicating substantial plastic deformation, was found across both cross-sections. The only significant trend was somewhat higher values of H_v in the vicinity of the fibrous reinforcement. This trend can be explained by a greater resistance to local plastic flow during the indentation process due to the close proximity of the fiber. No conclusive evidence of a tri-axial stress condition or of a high residual stress level was detected in either cross-section. It appears that massive plastic deformation (during stage III) in the region between points of load application has obscured any meaningful data in this area. This excessive plastic deformation can be attrib-uted to extreme fiber ductility. It is suggested that in future studies termination of tensile stress after completion of stage II deformation would allow more meaningful data to be obtained in this cross-sectional area.

Composite Fracture

The principles of composite action require that suffi-cient tensile stress be developed in the fibrous reinforcement

to cause fracture. This requirement must be satisfied if the metal matrix composite is to reach its full strength potential. A secondary requirement is that fiber fracture should occur prior to failure of the metallic matrix. This condition brings about two benefits: (1) as fibers begin to fracture, segments of broken fiber still retain their bond with the matrix, acting as short discontinuous reinforcement, and (2) after all fibers fracture, the ductile metal matrix is still able to carry some proportionate part of the load, hence preventing immediate catastrophic failure of the composite. The 3-fiber model system and the 5-fiber model system developed in this study adhere to the two principles discussed above. This is supported by the load-deformation curves shown in Figures 15 and 16. As mentioned previously, the aluminum/stainless steel composite fabricated by the Harvey Engineering Laboratories of Torrance, California served as the basis for much of the development of these model systems. It is therefore interesting to compare a fracture surface micrograph of the Harvey composite with similar micrographs of the model systems. These micrographs are shown in Figures 20 - 22.

Of primary importance in the development of metal matrix composites are the high values of ultimate tensile strength which can be achieved. Composite performance can be evaluated on the basis of rule-of-mixtures predictions of ultimate

tensile strength. Kelly [22] states that such predictions
are actually a theoretical lower limit for continuous-fiber
composites. This can be justified on the basis of a tri-
axial state of stress in the matrix. The higher modulus
fibers will exert a restraining effect on the matrix under
uniaxial load, thereby creating triaxial stresses. The result
will be a decrease in matrix deformation and a corresponding
increase in the yield strength, ultimate strength, and modulus
of the matrix [7]. Furthermore, synergistic behavior is
common in the case of ductile fiber composites where fiber-
matrix bonding serves as a deterent to localized plastic
instability, or "necking".

The measured ultimate tensile strengths for the model
systems were as follows: 12,350 psi. for the 3-fiber model
and 15,100 psi. for the 5-fiber model. Predicted ultimate
strength values were determined from the relationship given
by equation (4) which gives ultimate strength values of
11,300 psi. for the 3-fiber model and 14,400 psi. for the
5-fiber model. It should be noted that for the purpose of
rule-of-mixtures predictions that the matrix stress when the
fibers are strained to their ultimate tensile strain is
assumed to equal the ultimate tensile strength of the matrix,
$(\delta_m)_{\varepsilon'_f} \simeq \delta_{mu}$. This assumption appears valid since the
ductile stainless steel fibers exhibit such a large amount of
elongation prior to fracture. Thus, it can be seen that actual

model system strengths exceed predicted rule-of-mixtures
strengths be approximately 9% and 5% for the 3-fiber model
and the 5-fiber model, respectively. It is apparent that
synergistic effects are present in both model systems.

An analysis of the effects of both matrix strain
hardening and triaxiality can be made if true stress, rather
than engineering stress, values are used at the ultimate
strength condition for the model systems. This approach is
necessitated since a substantial reduction in area occurs
in the model systems prior to the end of stage III deformation.
Using an estimate of the actual composite cross-sectional
area at the point of fiber fracture, the following data can be
produced:

3-FIBER MODEL:	End of Stage I Deformation	Ultimate Strength Condition Based on True Stress
Composite Stress	6,725 psi.	16,300 psi.
Fiber Stress	18,700*	127,000
Matrix Stress	6,225*	11,800

5-FIBER MODEL:	End of Stage I Deformation	Ultimate Strength Condition Based on True Stress
Composite Stress	8,400 psi.	19,900 psi.
Fiber Stress	22,300*	127,000
Matrix Stress	7,450*	12,450

* Determined by ratio of elastic moduli [21].

The above data show a significant increase in the matrix
stress level at the end of stage I deformation. Values of
6,225 psi. and 7,450 psi. for the 3-fiber and 5-fiber models,
respectively, are considerably above the 2,900 psi. yield
stress that would be expected at this point. This is indic-
ative of substantial triaxiality in the model systems. The
ultimate matrix stress levels for the models are both higher
than the uncomposited U.T.S. of 8,750 psi. (true stress) for
high purity aluminum. This is further evidence of triaxial
stress conditions. The large increase in matrix stress in
going from the end of stage I to fracture not only confirms
triaxiality but also shows the effects of considerable
matrix strain hardening. It should be noted also that the
matrix stress for the 5-fiber model is higher than for the
3-fiber model both at the end of stage I and at ultimate
strength conditions. This can be attributed to greater tri-
axial restraint in the 5-fiber model.

V.   CONCLUSIONS

The objectives of this research program in the field
of metal matrix composites have been met. A continuous-
fiber model system has been developed by combining large
diameter stainless steel fibers, or rods, with a matrix of
high purity aluminum. The 3-fiber and 5-fiber models meet
the following four criteria for a valid model system: (1) a
stress-strain behavior which compares closely with actual
metal matrix composite systems, (2) a mode of failure which
is the same as ideal composite failure, i.e., fiber fracture
followed by matrix failure, (3) favorable comparison with
rule-of-mixtures strength predictions, and (4) the generation
of fiber tensile stress through the mechanism of matrix shear
stress transfer rather than through any direct axial stress on
the fibers.

The validity of the large fiber model system has been
substantiated through qualitative studies of the stress-strain
behavior and the mode of failure. The characteristic four-
stage composite stress-strain behavior can be clearly seen
on the load-deformation curve for both model systems. Failure
occurs by the fracture of the stainless steel fibers followed
by failure of the pure aluminum matrix. The method of uni-
axial loading used in this work employs shoulder grips which
apply direct stress only to the aluminum matrix. Fiber

tensile stresses are developed solely by the transfer of shear stress across the fiber-matrix interfacial region. It is significant to note that the aluminum/stainless steel model system exhibits synergistic performance which is commonly found in well-fabricated fiber reinforced metals. The 3-fiber model system exceeded traditional rule-of-mixtures strength predictions by approximately 9%, the 5-fiber system by 5%.

Deformation studies have been carried out through the use of microhardness techniques to measure strain hardening in the pure aluminum matrix. This work not only served to confirm the validity of the model system but also permitted study of the behavior of the metallic matrix under loading, that is, during shear stress transfer. A significant increase in Vicker's Hardness Number of the aluminum matrix was found near the ends of the stainless steel fibers. The hardness data support the contention that fiber tensile stress was indeed developed through the mechanism of shear stress transfer in the matrix. High values of matrix shear stress are expected near fiber ends in order to develop tensile stress in the fibrous reinforcement.

The observation of little change in matrix hardness as a function of radial distance from the fibers confirms earlier work done with commercially available, small-size metal matrix composite systems.

REFERENCES

1. Jones, R.C., "Structural Metal Composites," Civil
    Engineering, ASCE, February, 1967, pp. 54-57.

2. Sutton, W.H., "Fiber-Reinforced Metals," Modern Compos-
    ite Materials, edited by Broutman, L.J. and Krock, R.H.,
    Addison-Wesley Publishing Company, Reading, Massachu-
    setts, 1967, pp. 412-441.

3. Adsit, N.R., "Metal Matrix Fiber Strengthened Materials,"
    GDC-ERR-AN-867, General Dynamics Convair, San Diego,
    California, December, 1965.

4. Wolff, E.G. and Hill, R.J., "Research on Boron Filament/
    Metal Matrix Composite Materials," Technical Report
    AFML-TR-67-140, June, 1967.

5. Price, D.E. and Wagner, H.J., "Preparation and Properties
    of Fiber-Reinforced Structural Materials," DMIC
    Memorandum 176, Battelle Memorial Institute, Columbus,
    Ohio, August, 1963.

6. Davis, L.W., "How Metal Matrix Composites Are Made," Paper
    presented at the ASTM/ASME Joint Symposium on Composites,
    Chicago, Illinois, November, 1966.

7. Burte, H.M., Bonanno, F.R. and Herzog, J.A., "Metal Matrix
    Composite Materials," Orientation Effects in the Mecha-
    nical Behavior of Anisotropic Structural Materials, ASTM
    STP 405, Am. Soc. Testing Mats., 1966, pp. 59-92.

8. Ebert, L.J., Hamilton, C.H. and Hecker, S.S., "Development
    of Design Criteria for Composite Materials," Technical
    Report AFML-TR-67-95, April, 1967.

9. Weeton, J.W. and Signorelli, R.A., "Fiber-Metal Composites,"
    Strengthening Mechanisms (Metals and Ceramics), Pro-
    ceedings of the Twelfth Sagamore Army Material Research
    Conference, Edited by Burke, J.J., Reed, N.L. and Weiss,
    V., Syracuse University Press, 1966, pp. 477-530.

10. Schuster, D.M., "Single and Multi-Fiber Interactions in
    Discontinuously Reinforced Composites," Ph.D. Thesis,
    Cornell University, Ithaca, New York, February, 1967.

11. Kaarlela, W.T., Margolis, W.S. and Thornton, H.R.,
     "Fundamental Study of Metal Matrix Composites," Paper
     presented to ASTM Symposium or Fiber Strengthened
     Metallic Composites, 1966 ASM National Metal Congress,
     Chicago, Illinois, November, 1966.

12. Kelly, A. and Davies, G.J., "The Principles of Fiber
     Reinforcement of Metals," Metallurgical Reviews, Vol.
     10, No. 37, 1965, pp. 1-77.

13. Parikh, N.M., "Deformation and Fracture in Composite
     Materials," IITRI-B6037-6 (Final Report), IIT Research
     Institute, Chicago, Illinois, 31 March 1966.

14. Tyson, W.R. and Davies, G.J., "A Photoelastic Study of the
     Shear Stresses Associated with the Transfer of Stress
     During Fiber Reinforcement," British Journal of Applied
     Physics, Vol. 16, 1965, pp. 199-205.

15. Kelly, A. and Tyson, W.R., "Tensile Properties of Fiber-
     Reinforced Metals: Copper/Tungsten and Copper/Molybdenum,"
     Journal of Mechanics and Physics of Solids, Vol. 13,
     1965, pp. 329-350.

16. Sumner, E.V., "Development of Ultra High Strength, Low
     Density, Aluminum Plate Composites," HA-2263 (Final
     Report), Harvey Engineering Laboratories, Torrance,
     California, July, 1966.

17. Brandt, J.L., "Properties of Pure Aluminum," Aluminum,
     Edited by Van Horn, K.R., Vol. I, American Society for
     Metals, Metals Park, Ohio, 1967, pp. 1-30.

18. Parr, J.G. and Hanson, A., An Introduction to Stainless
     Steel, American Society for Metals, Metals Park, Ohio,
     1966.

19. Broutman, L.J. and Krock, R.H., "Principles of Composites
     and Composite Reinforcement," Modern Composite Materials,
     edited by Broutman, L.J. and Krock, R.H., Addison-
     Wesley Publishing Company, Reading, Massachusetts, 1967,
     pp. 3-26.

20. MacFayden, D.J. and Jones, R.C., "Structural Aspects of
     Metal Matrix Composites," Research Report R67-64,
     Massachusetts Institute of Technology, Cambridge,
     Massachusetts, December, 1967.

21. Jones, R.C., "Deformation of Wire Reinforced Metal Matrix
     Composites," Research Report P67-10, Massachusetts
     Institute of Technology, Cambridge, Massachusetts, June,
     1967.

22. Kelly, A., <u>Strong Solids</u>, Clarendon Press, Oxford, 1966.

SHEAR STRESS

TENSILE STRESS

L = 1.5 L$_c$/2

FIBER U.T.S.

L = L$_c$/2

FIBER U.T.S.

L = 0.75 L$_c$/2

FIBER U.T.S.

L = 0.5 L$_c$/2

FIBER U.T.S.
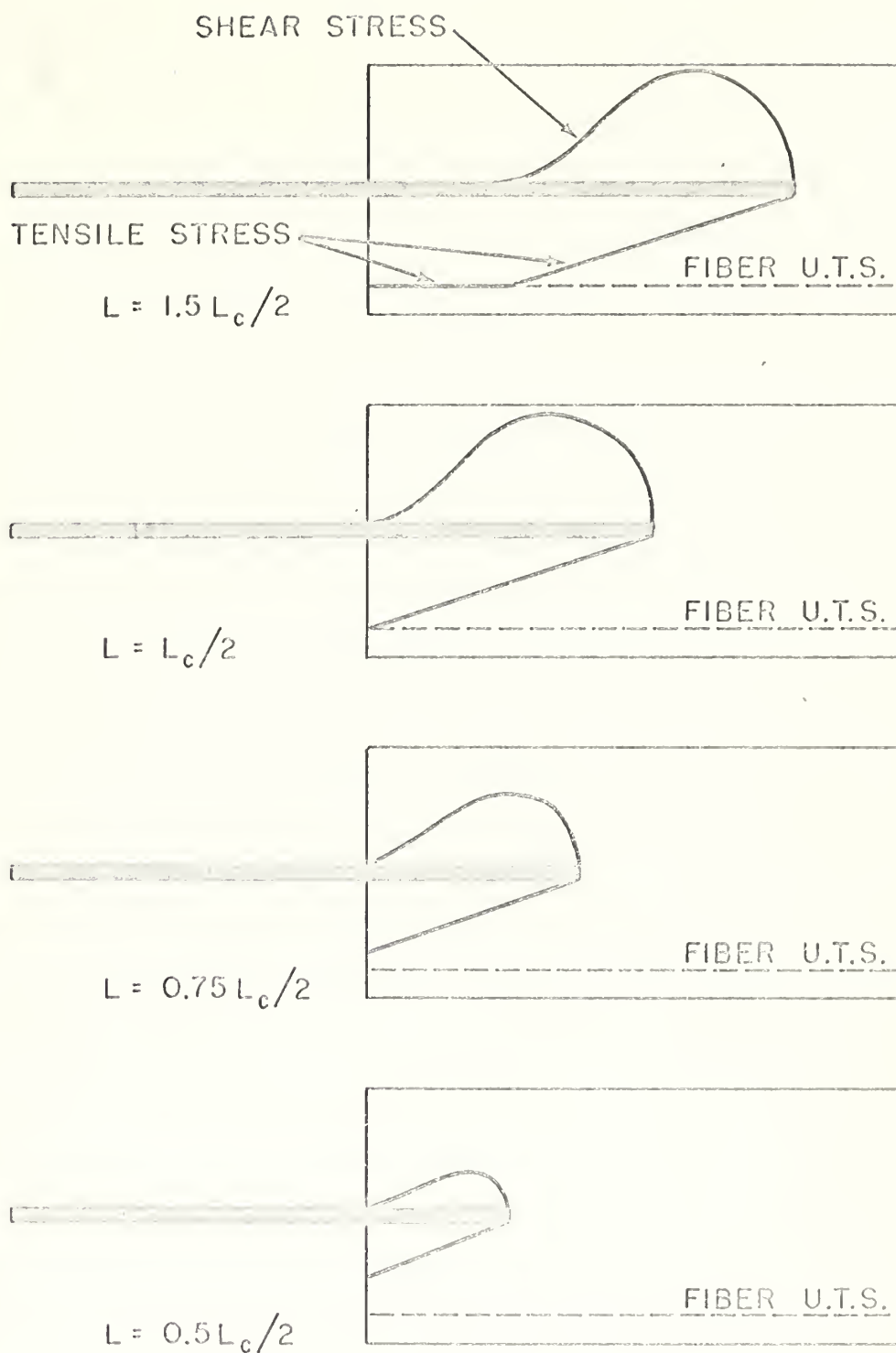
FIGURE I.   SCHEMATIC REPRESENTATION OF INTERFACIAL SHEAR STRESS
AND FIBER TENSILE STRESS ALONG FIBER AXIS FOR VARIOUS
DEPTHS OF FIBER EMBEDMENT

-49-

FIGURE 2.   TWO VIEWS OF A PULL-OUT TEST SPECIMEN PRIOR TO TESTING
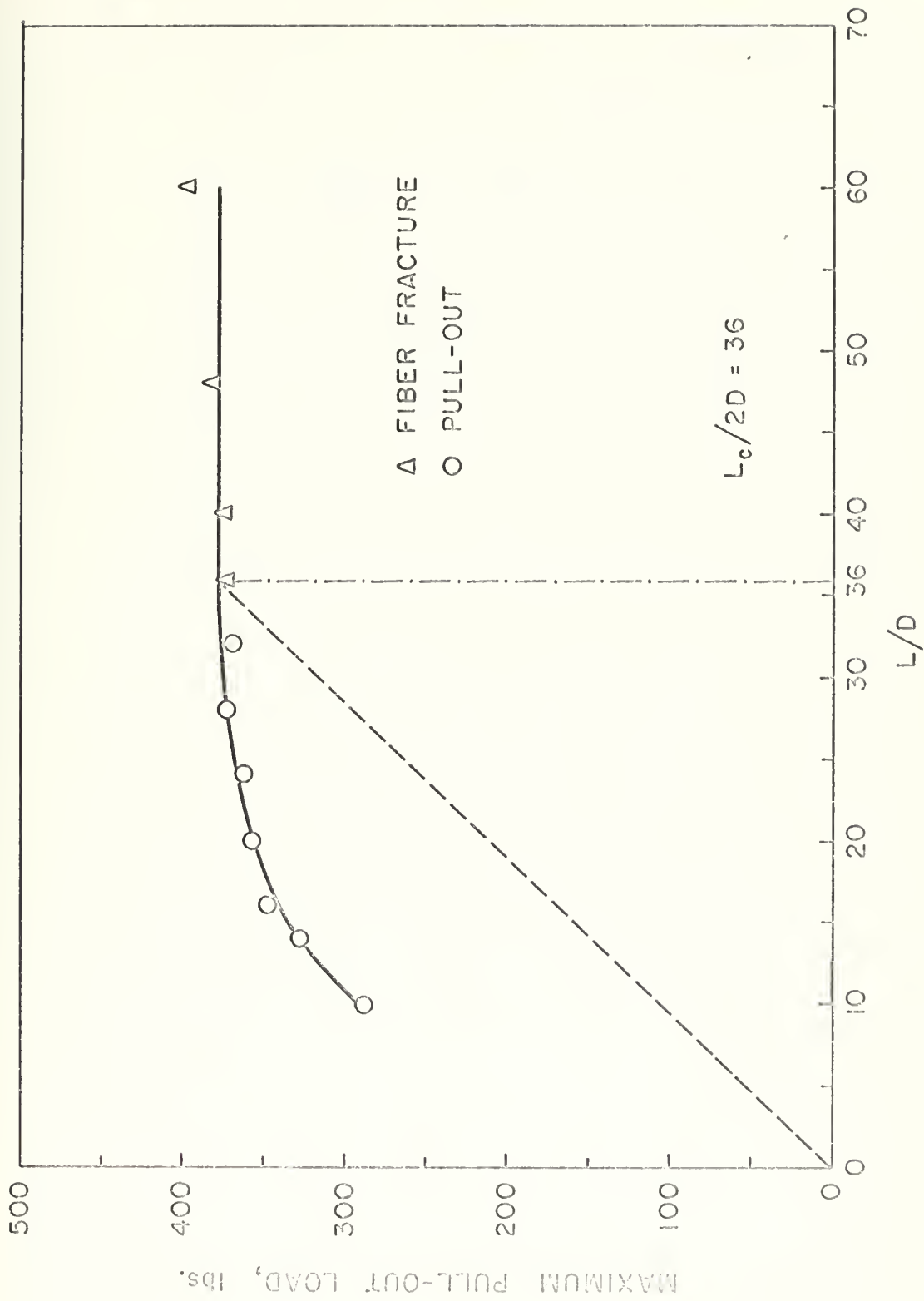
FIGURE 3. PLOT OF MAXIMUM PULL-OUT LOAD VS. LENGTH/DIAMETER RATIO

MATRIX

FIBER

$V_F = 3.9\%$

0.55" DIAMETER

$\frac{1"}{16}$

$V = 6.5\%$
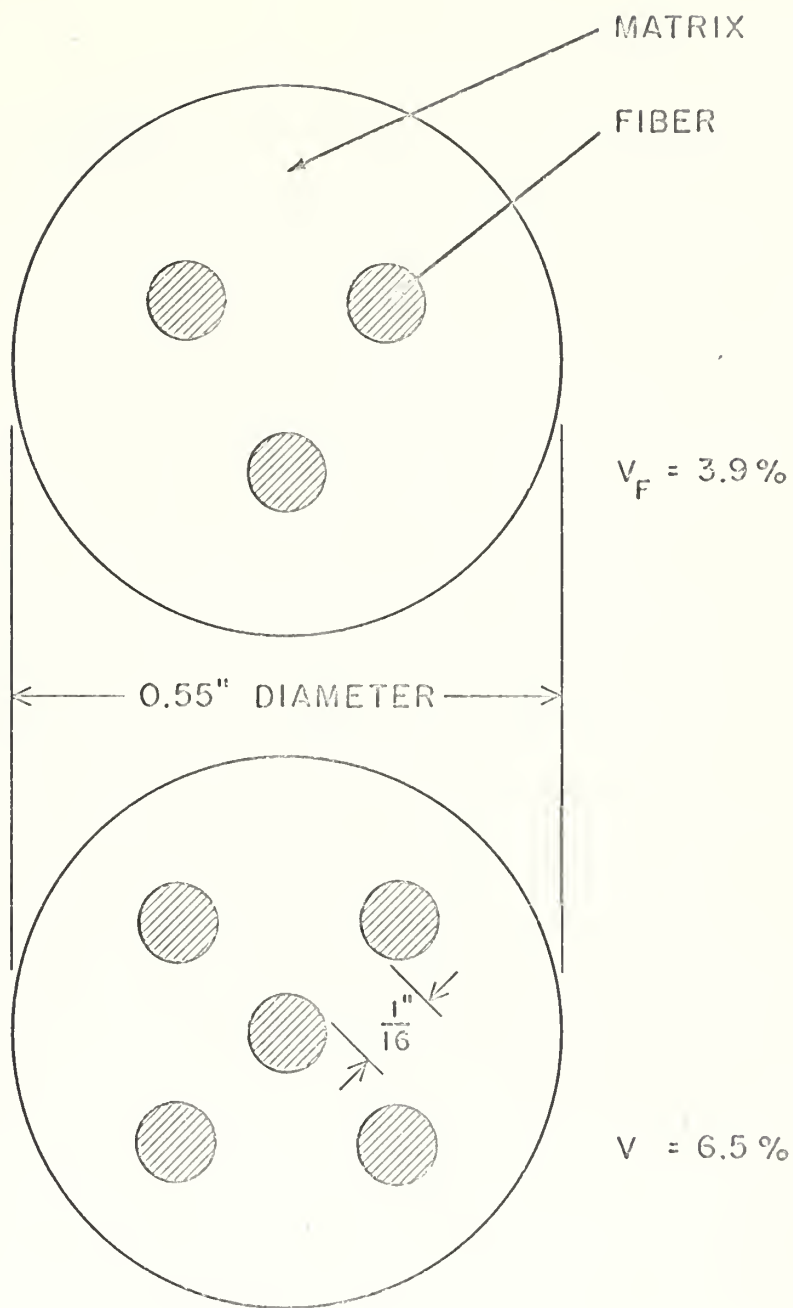
FIGURE 4.   CROSS-SECTION DESIGN OF 3-FIBER AND 5-FIBER
            MODEL SYSTEMS
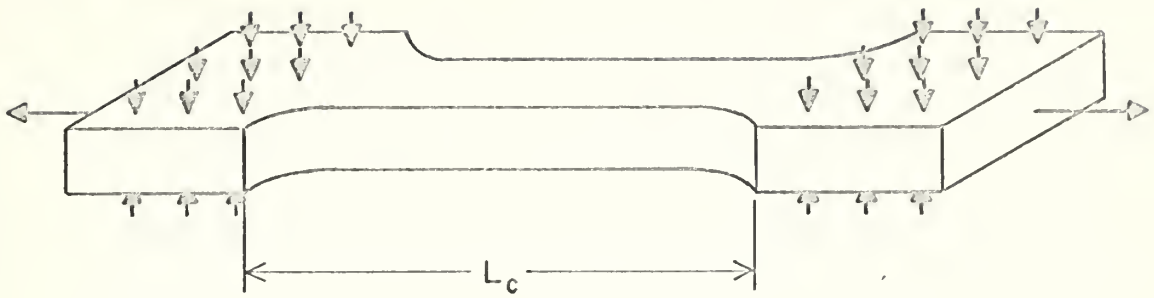
(A)
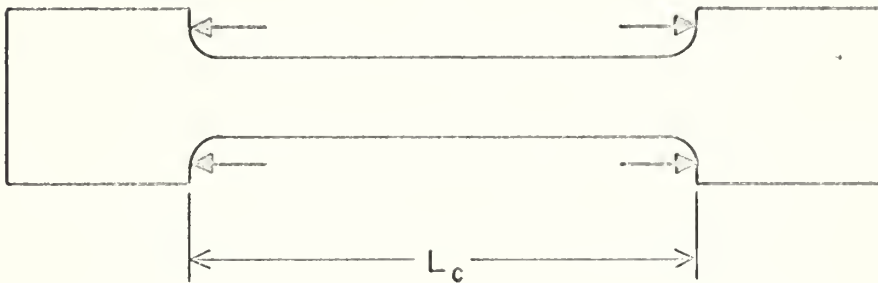
(B)
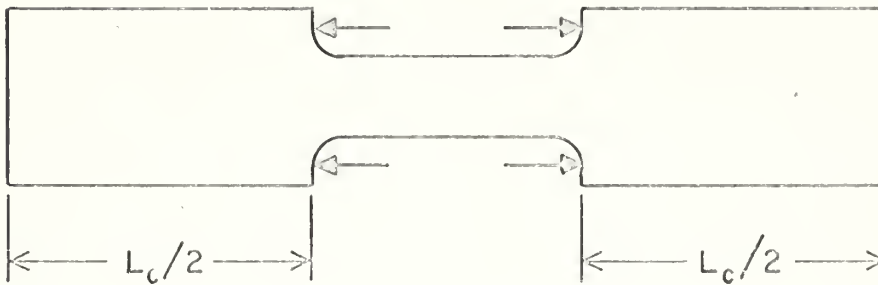
(C)

FIGURE 5. STEPS IN THE DEVELOPMENT OF THE MODEL SYSTEM DESIGN. NOTE HEAVY ARROWS INDICATING THE NATURE OF THE APPLIED LOADING.
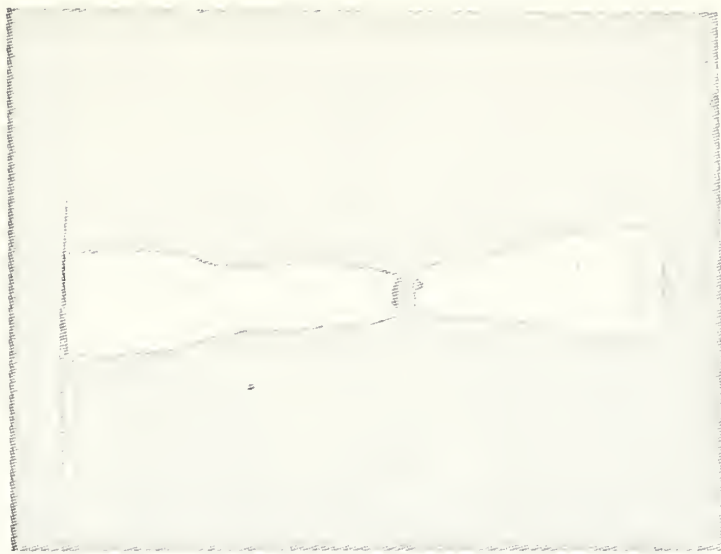
FIGURE 6.   FAILURE MODE OF SEVERAL IMPROPERLY DESIGNED CONTINUOUS-
FIBER MODEL SYSTEMS. SPECIMEN TESTED WITH CONVENTIONAL
GRIPS SHOWN AT TOP. SPECIMENS TESTED WITH SHOULDER GRIPS
SHOWN AT BOTTOM.

FIGURE 7. FINAL MODEL SYSTEM DESIGN PRIOR TO TESTING (TOP)
AND AFTER FRACTURE (BOTTOM)
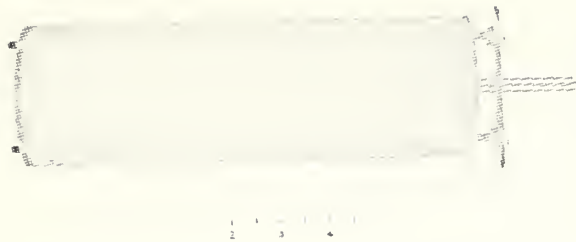
SIDE VIEW OF MOLD
FOR CASTING MODEL
SYSTEMS

TOP VIEW OF MOLD
FOR CASTING MODEL
SYSTEMS

TOP VIEW OF MOLD
FOR CASTING PULL-
OUT SPECIMENS

FIGURE 8.   GRAPHITE MOLDS USED IN GRAVITY CASTING OPERATION

FIGURE 9. ETCHED CROSS-SECTION OF 3-FIBER MODEL SYSTEM (5X)
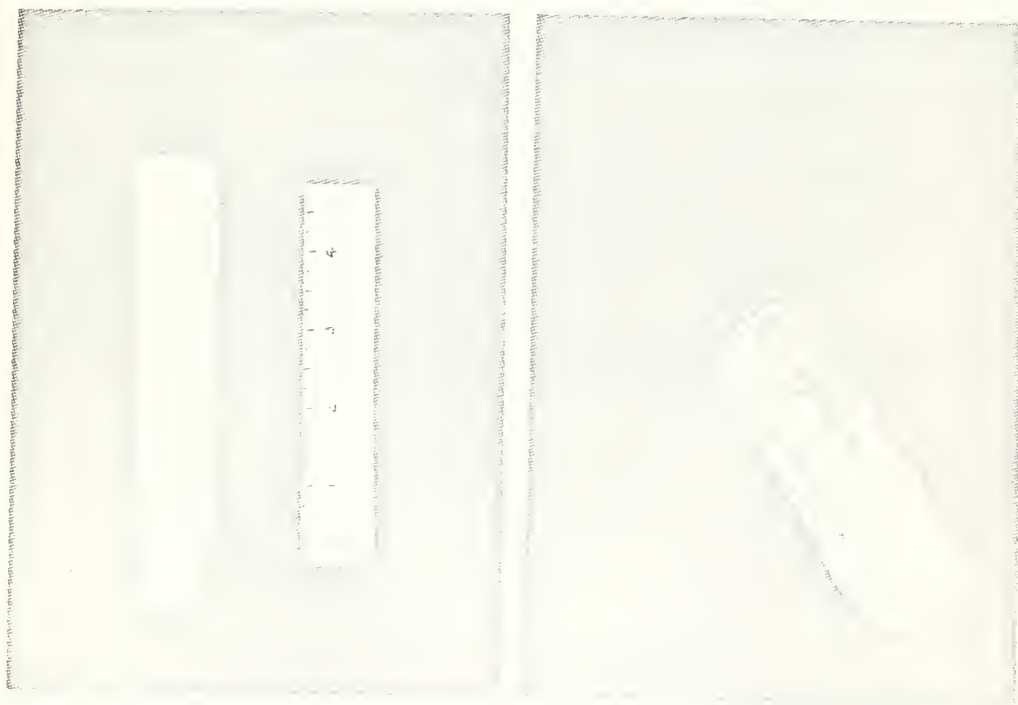
FIGURE 10. CONTINUOUS-FIBER MODEL (LEFT) AND PULL-OUT TEST
SPECIMEN (RIGHT) IN AS-CAST CONDITION
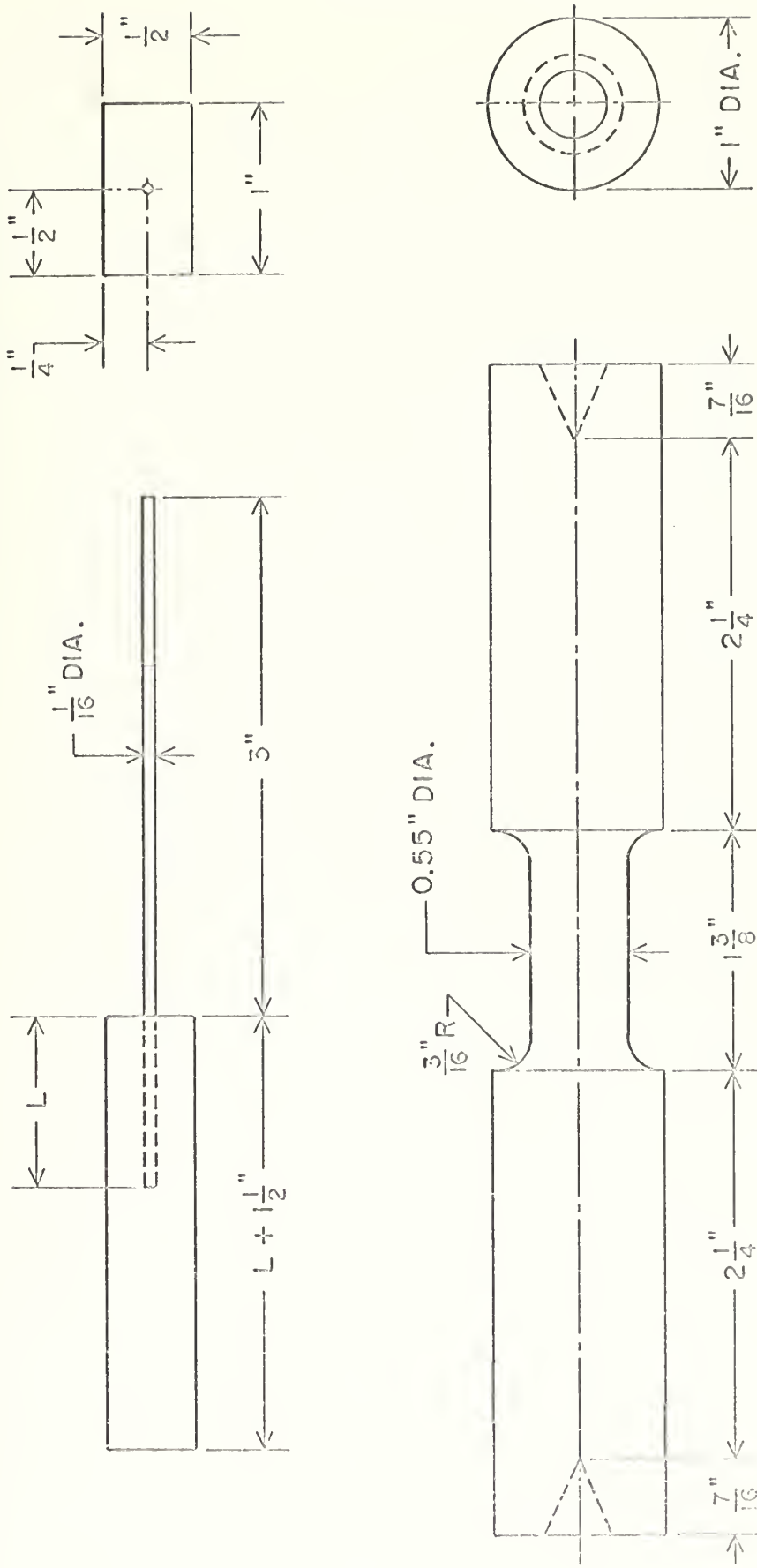
FIGURE 11. SCALED DRAWINGS OF CONTINUOUS-FIBER MODEL (BOTTOM) AND PULL-OUT TEST SPECIMEN (TOP)
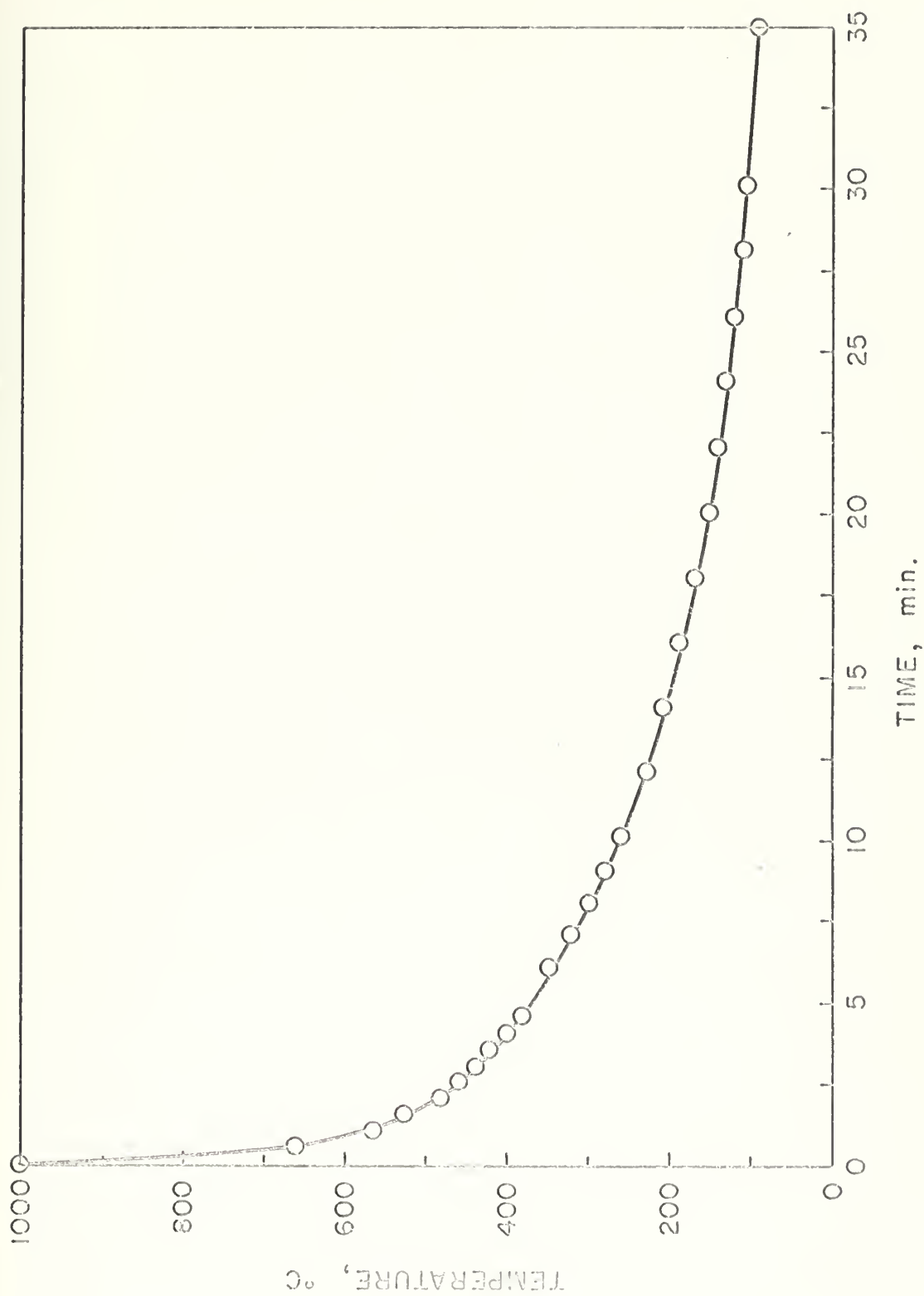
FIGURE 12. CURVE OF FIBER TEMPERATURE VS. TIME DURING THE GRAVITY CASTING OPERATION
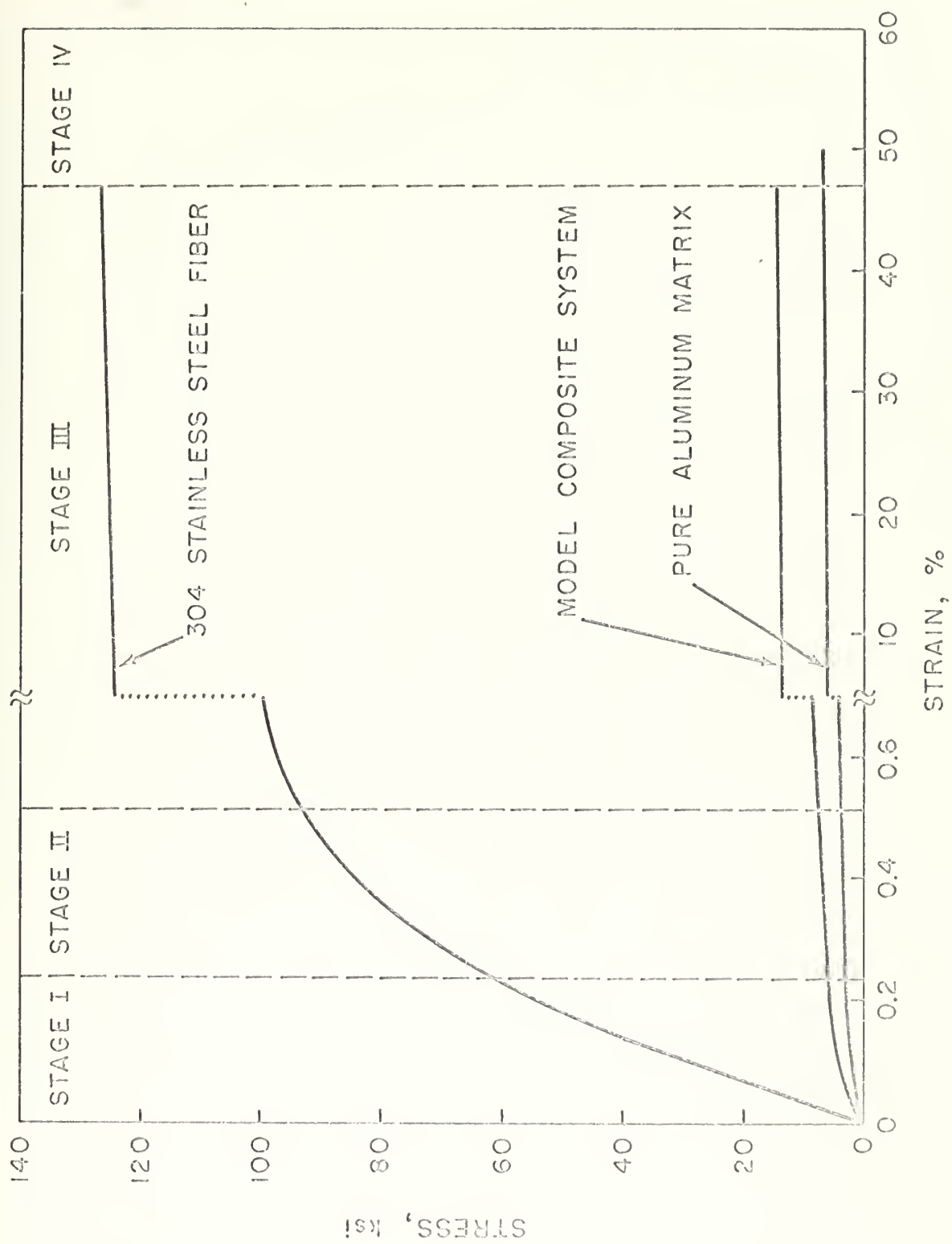
FIGURE 13. SCHEMATIC REPRESENTATION OF THE 4 STAGES OF COMPOSITE DEFORMATION

FIGURE 14. ONE END OF A CONTINUOUS-FIBER MODEL SYSTEM
IN A SHOULDER GRIP
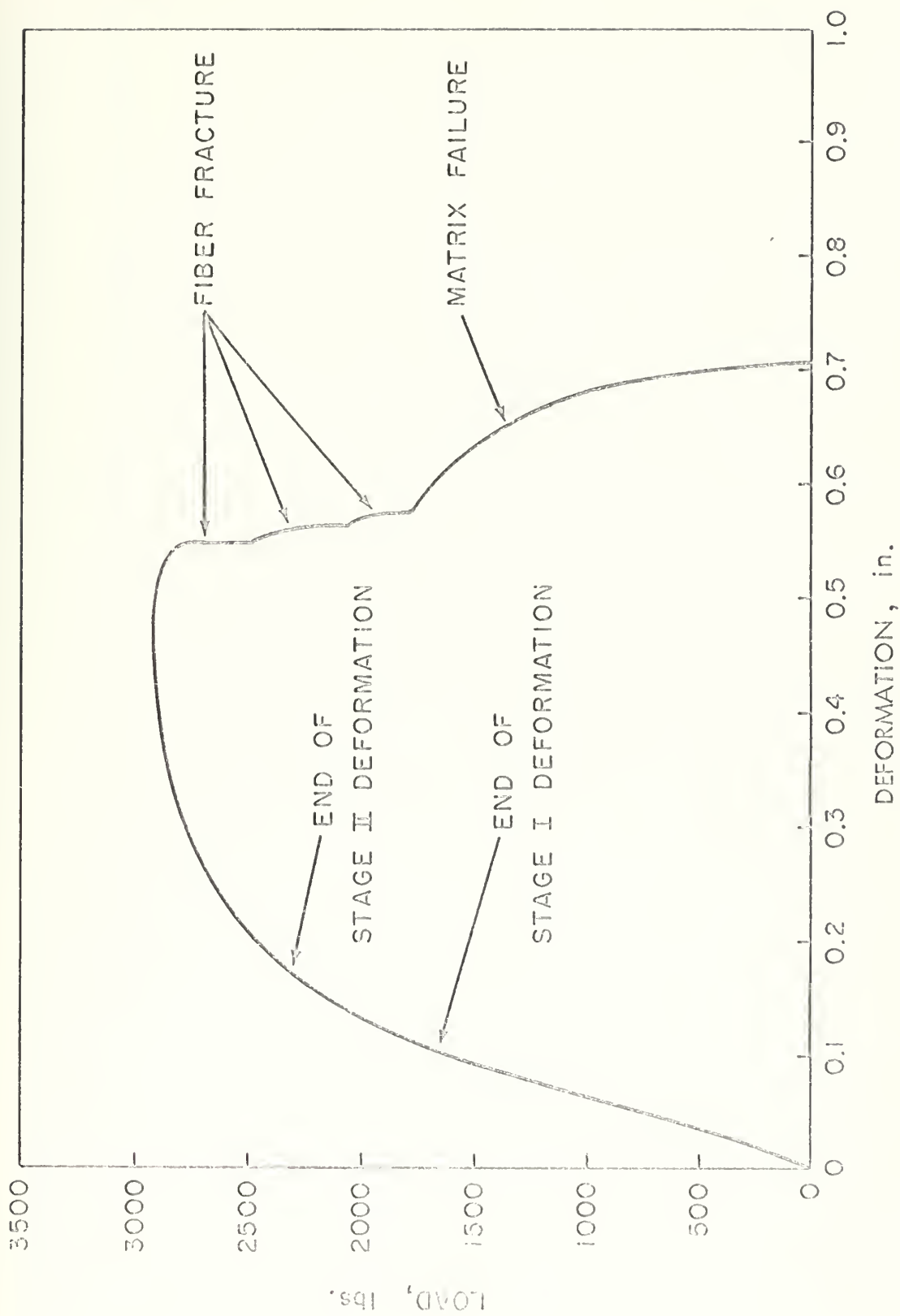
FIGURE 15. LOAD-DEFORMATION CURVE FOR 3-FIBER MODEL SYSTEM
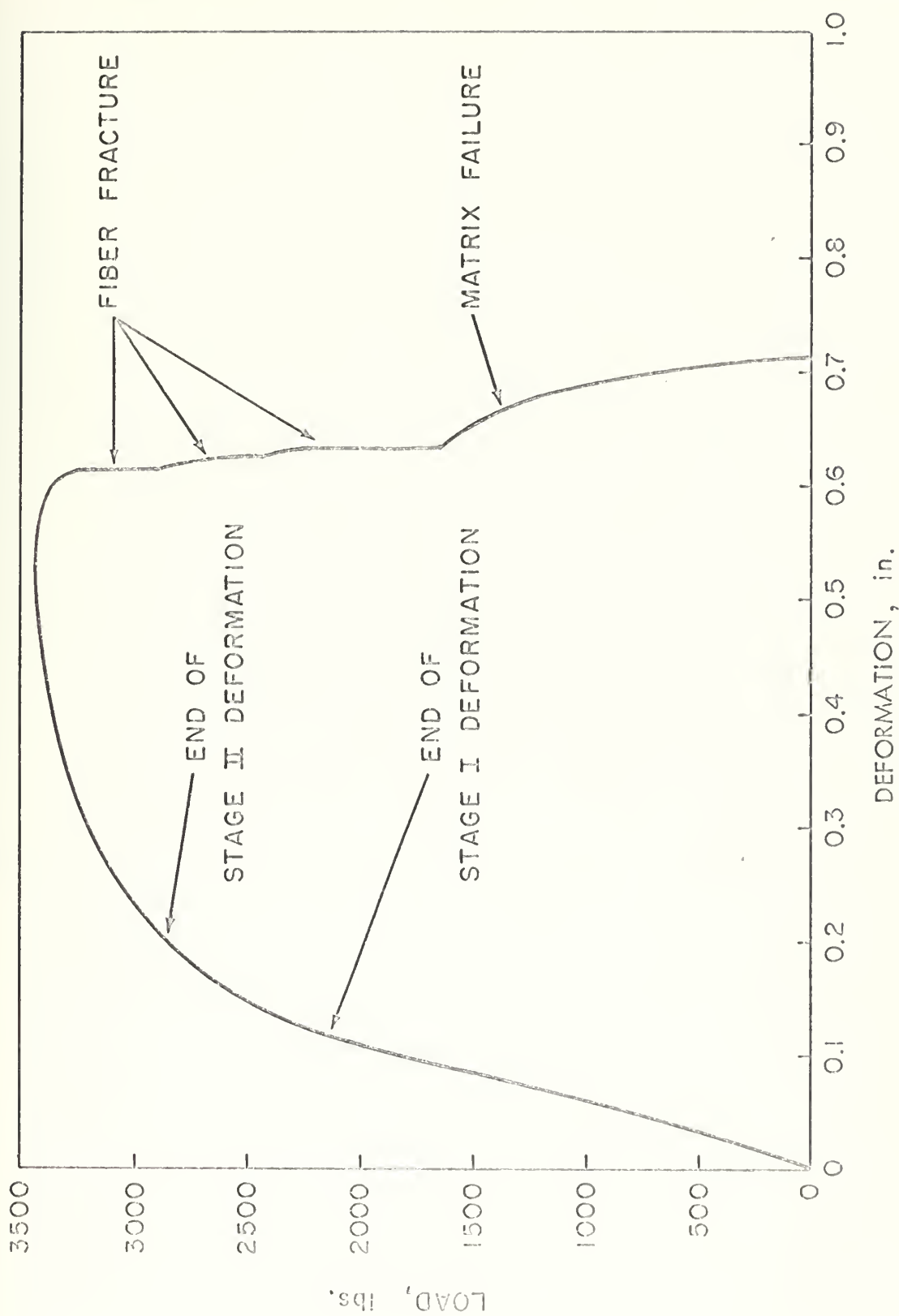
FIGURE 16.   LOAD-DEFORMATION CURVE FOR 5-FIBER MODEL SYSTEM

FIGURE 17.   CLUSTER OF FOUR MICROHARDNESS INDENTATIONS USED
              TO DETERMINE THE VICKER'S HARDNESS NUMBER (500X)

MATRIX

EXPOSED FIBER

FIBER BELOW SURFACE

$L_c/2$

(NOT TO SCALE)

O REPRESENTS AREAS IN WHICH
  INDENTATIONS WERE MADE
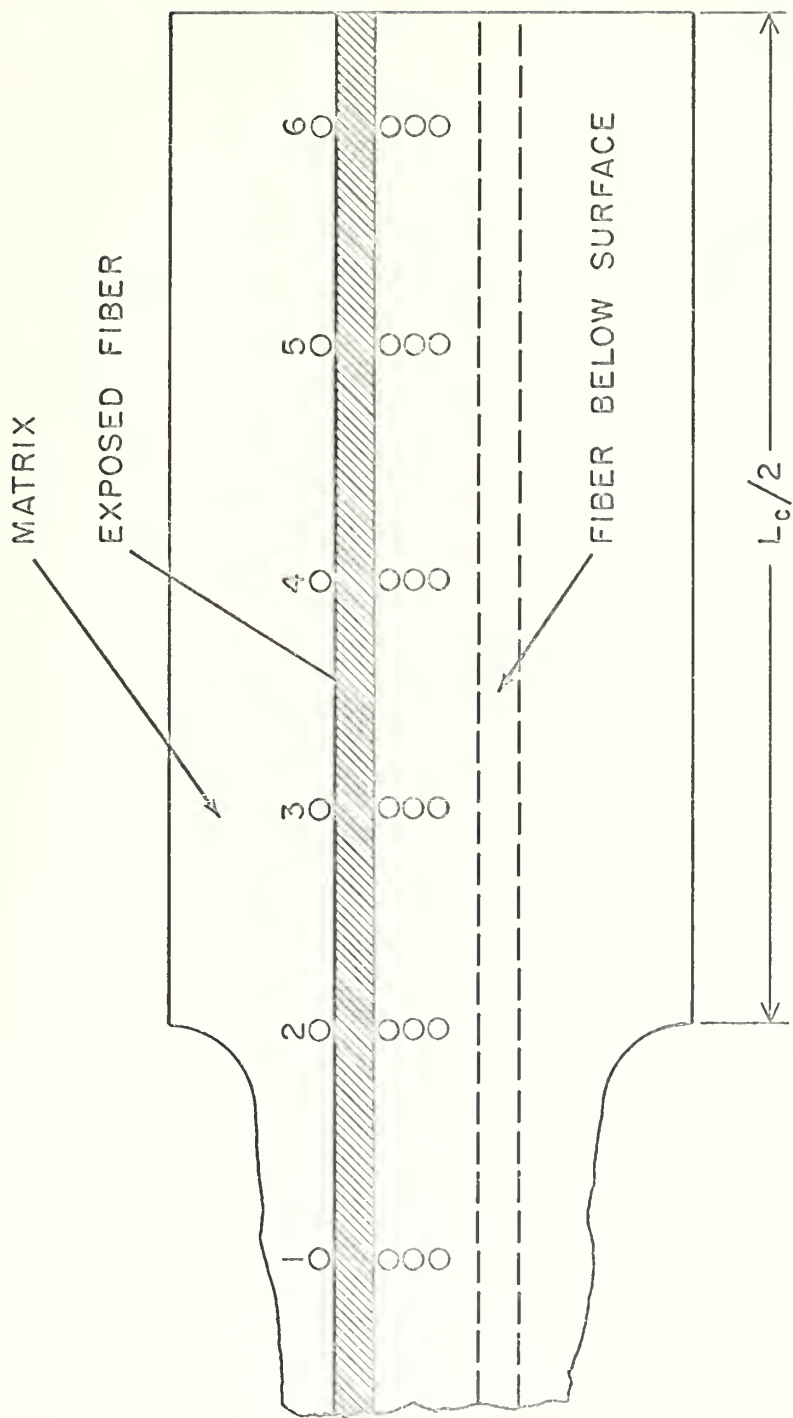
FIGURE 18.   LONGITUDINAL SECTION OF FRACTURED MODEL SYSTEM SHOWING
             AREAS IN WHICH MICROHARDNESS INVESTIGATIONS WERE MADE
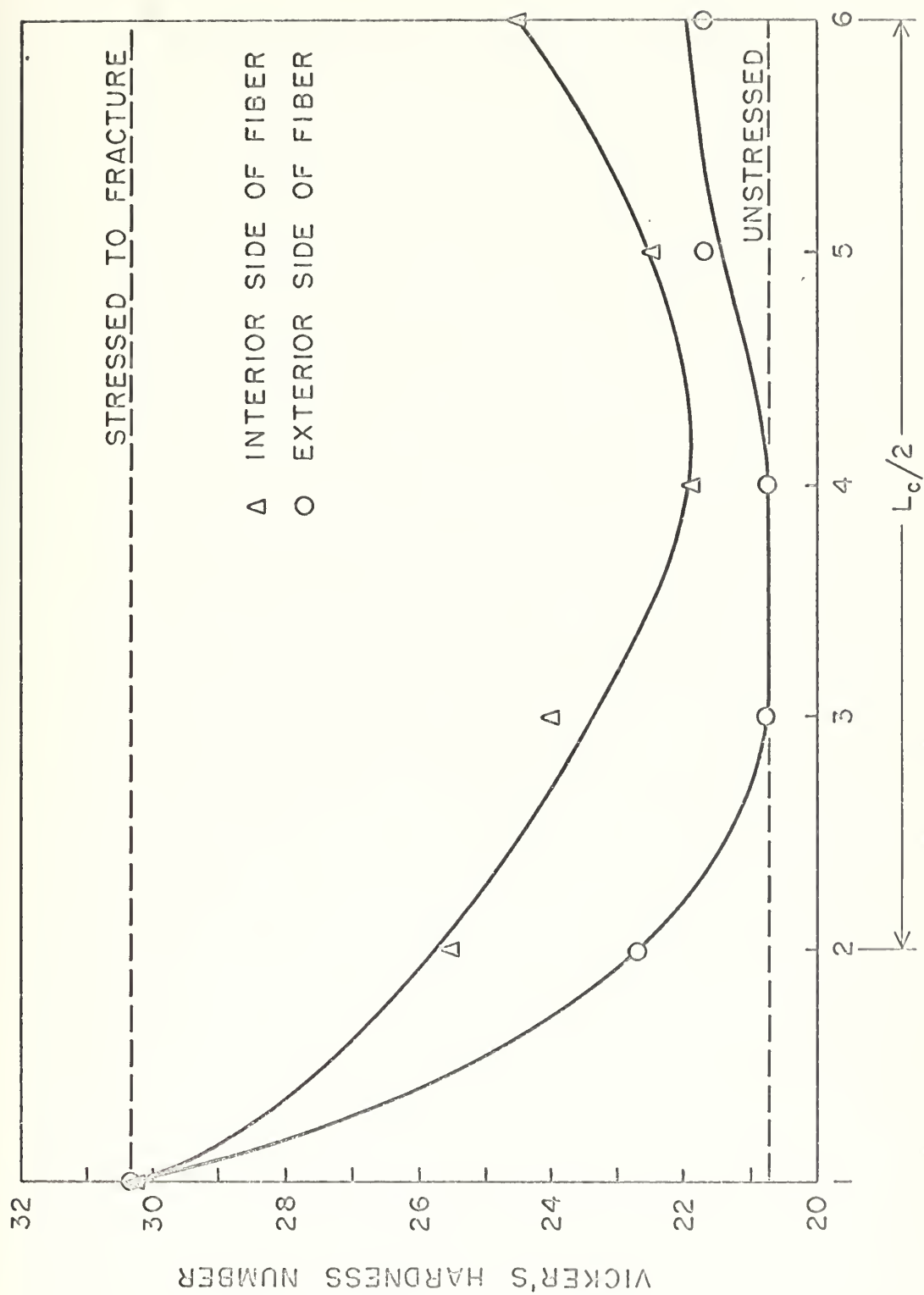
FIGURE 19. VICKER'S HARDNESS NUMBER PLOTTED AS A FUNCTION
OF DISTANCE ALONG THE FIBER AXIS

FIGURE 20. FRACTURE SURFACE OF 3-FIBER MODEL SYSTEM VIEWED
AT 45° (TOP) AND 90° (BOTTOM)(5X)

FIGURE 21. FRACTURE SURFACE OF 5-FIBER MODEL SYSTEM VIEWED
AT 45° (TOP) AND 90° (BOTTOM)(5X)
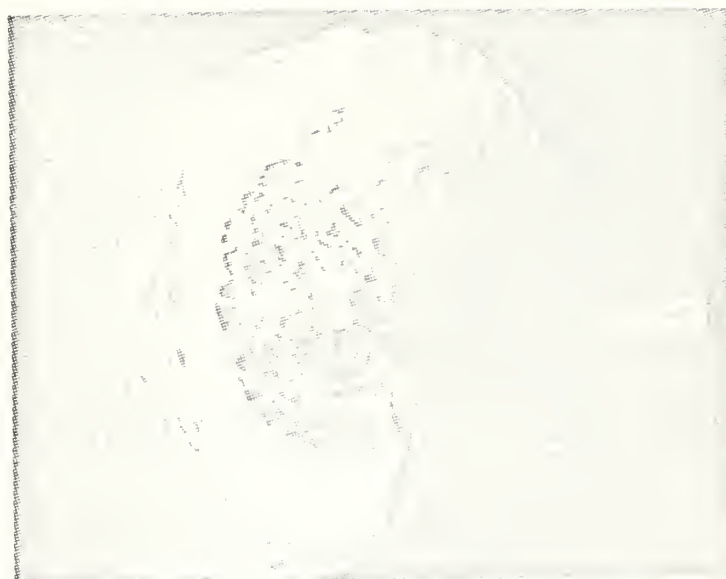
FIGURE 22. SCANNING ELECTRON MICROGRAPH OF FRACTURE SURFACES OF A COMMERCIAL 2024 ALUMINUM/NS355 STAINLESS STEEL COMPOSITE (.004" FIBERS). TOP MICROGRAPH VIEWED AT 45°; BOTTOM MICROGRAPH SHOWS "CUP AND CONE" FRACTURE SURFACE OF A SINGLE FIBER.

Appendix

LIST OF FIGURES